Journal of the Korean Society for Nondestructive Testing
Vol. 26, No. 3 (2006. 6)

Effects of Material Anisotropy on Ultrasonic Beam Propagation: Diffraction and Beam Skew

Hyunjo Jeong*,† and Lester W. Schmerr, Jr.**

Abstract The necessity of nondestructively inspecting austenitic steels, fiber-reinforced composites, and other inherently anisotropic materials has stimulated considerable interest in developing beam models for anisotropic media. The properties of slowness surface play a key role in the beam models based on the paraxial approximation. In this paper, we apply a modular multi-Gaussian beam (MMGB) model to study the effects of material anisotropy on ultrasonic beam profile. It is shown that the anisotropic effects of beam skew and excess beam divergence enter into the MMGB model through parameters defining the slope and curvature of the slowness surface. The overall beam profile is found when the quasilongitudinal (qL) beam propagates in the symmetry plane of transversely isotropic austenitic steels. Simulation results are presented to illustrate the effects of these parameters on ultrasonic beam diffraction and beam skew. The MMGB calculations are also checked by comparing the anisotropy factor and beam skew angle with other analytical solutions.

Keywords: Anisotropic Materials, MMGB Model, Slowness Surface, Beam Diffraction/Skew

1. Introduction

Multi-Gaussian beam (MGB) models can be used to describe the propagation of ultrasonic beams from planar or focused transducers in a variety of testing situations (Schmerr, 2000; Rudolph, 1999; Song et al., 2004; Kim et al., 2004). One of the attractive features of MGB models is that they are numerically very efficient. This is because these models rely on the superposition of a small number (10-15) of Gaussian beams whose properties can be described in analytical terms even after propagation through general anisotropic media and after interactions with multiple curved interfaces. The MGB models also form an important part of more complete ultrasonic measurement models that can simulate the measured response of defects. In these measurement models, the MGB models are used to predict diffraction correction terms which account for the effects of the acoustic wave fields as they travel from the transducer to the defect and back. (Kim et al. 2004; Lopez-Sanchez 2006). As the number of interfaces increases, however, the analytical expressions for the amplitude and phase of a Gaussian beam become increasingly complex. Modular multi-Gaussian beam (MMGB) models (Schmerr and Sedov 2003) have been developed as an alternative approach. The MMGB model provides an efficient formulation for ultrasound propagation because of its modular matrix form after multiple interface interactions. This modular way of expressing the solution is very convenient to generalize for N transmissions/reflections by representing the propagating Gaussian amplitude

Received: May 15, 2006, Accepted: June 15, 2006. * Division of Mechanical and Automobile Engineering, Wonkwang University, Iksan, Jeonbuk 570-749, Korea, ** Center for Nondestructive Evaluation and Department of Aerospace Engineering, Iowa State University, Ames, IA 50011, USA, † Corresponding author: hjjeong@wonkwang.ac.kr

and phase in terms of the global matrices for the entire set of multiple propagation and transmission/reflection matrices. The MMGB models were used to calculate the ultrasonic beam profiles for a multilayered isotropic medium with interface curvatures (Huang et al. 2005) and for a contact/angle beam testing (Jeong et al. 2005).

The necessity of nondestructively inspecting austenitic steels, fiber-reinforced composites, and other inherently anisotropic materials has stimulated considerable interest in wave propagation in anisotropic media. The properties of slowness surface play a key role in the beam models based on the paraxial approximation. The essential feature of this approximation is a Taylor series expansion of the slowness surface in the vicinity of the propagation direction. It is well known that the coefficients of the first- and second-order terms in the expansion of the slowness surface govern the beam skew and divergence respectively. The parameters A and B define the rate of change of slowness with propagation direction, and, hence, determine the group velocity and its direction. This effect is often referred to as beam skew. The parameters C, D, and E define the curvatures of slowness surface. As will be seen, these will determine the rate of divergence or convergence of the beam due to diffraction. Methods for calculating the group velocity components to determine beam skewing effects are readily available. The beam skew angle is given by $\cos\psi = 1\sqrt{A^2+B^2+1}$ and the group velocity is $\sqrt{A^2+B^2+1}$ larger than the phase velocity. The fact that the diffraction in an anisotropic material is related to that in an isotropic material by an "anisotropy factor" has been noted by several authors (Newberry and Thompson, 1989; Norris, 1987; Papadakis, 1964 and 1966). This factor can be thought of as the equivalent distance needed to be traveled in an isotropic medium to achieve the same diffraction effects that occur when traveling a distance in the anisotropic medium. The anisotropy factor is related to the second derivative of the slowness, so the curvature of the slowness surface controls the rate of beam spread. The anisotropy factor can be compared with the divergence parameter of Ogilby (Ogilvy 1986) and the distance scaling factor of Szabo and Slobodnik (Szabo and Slobodnik 1973). In our extension of the MMGB model to anisotropic materials, the anisotropic effects of beam skew and excess beam divergence also enter into the solution through the parameters A-E.

In this paper, we briefly describe a highly modular multi-Gaussian beam model that can be efficiently used to simulate the propagation of ultrasonic beams in an anisotropic solid. We illustrate the effects that changes in the slowness surface curvatures have on an ultrasonic transducer beam radiating into an anisotropic solid through the use of the MMGB model, where the field radiated by a transducer is modeled as the superposition of 10 Gaussian beams. Simulation results are presented for an austenitic steel when the quasilongitudinal (qL) wave propagates in the symmetry plane of this material. In order to check the MMGB prediction for the anisotropy factor, we set the parameters A-E to be zero for the isotropic solid in which the slowness is equivalent to S_0 for the anisotropic case.

2. A Modular Gaussian Beam Model

We will describe the modular Gaussian approach for the contact setup shown in Fig. 1 where a Gaussian beam is radiated at normal incidence through a planar anotropic solid interface. For the geometry of Fig. 1, we will assume that a Gaussian velocity profile is present at the transducer and propagates as a Gaussian beam into the solid. In Fig. 1, V(0) and **M**(0) are the known starting amplitude and phase values in the Gaussian at the transducer location.

When the incident Gaussian beam strikes a general anisotropic solid, a quasi L-wave and two quasi S-waves (qS_1, qS_2) will be generated and

propagated. In order to describe the transmitted waves in the solid we employ the coordinates (x_1, x_2, x_3). The x_3 coordinate is taken along the direction of the slowness vector in the anisotropic solid and (x_1, x_2) are coordinates orthogonal to the x_3 axis, with x_1 in the plane of incidence and x_2 normal to that plane. The propagation distance $\tilde{x}_3$ is measured in the x_3 direction along the central axis of the Gaussian beam.

When the beam propagates in the nonsymmetry directions, we introduce another coordinates (y_1, y_2, y_3) to describe the beam propagation in terms of the group velocity. The y_3 axis is taken along the group velocity direction and y_1 - y_2 plane is taken as the plane of incidence. The distance $\tilde{y}_3$ is measured along the y_3 axis. The beam skew is measured as an angle between y_3 and x_3 axes. For the case of beam propagation in the symmetry directions, the two coordinate systems coincide.

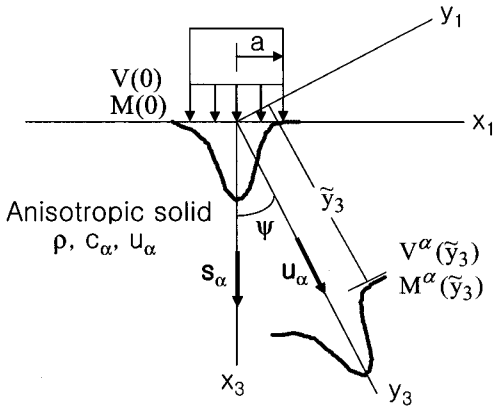

Fig. 1 A Gaussian beam propagation in a general anisotropic solid. Only one of three possible propagating waves is shown. The x_3 coordinate is taken along the direction of the slowness vector, $\mathbf{s}_\alpha$, in the anisotropic solid. For the beam propagation in nonsymmetry directions, y_3 axis is taken along the group velocity direction, $\mathbf{u}_\alpha$, and y_1-y_2 plane is taken as the plane of incidence. The distance $\tilde{y}_3$ is measured along the y_3 axis. The beam skew is measured as an angle between y_3 and x_3 axes.

2.1 Gaussian Beam Propagation in an Anisotropic Solid

The velocity amplitude $V^\alpha(\tilde{y}_3)$ and phase $\mathbf{M}^\alpha(\tilde{y}_3)$ of a propagating Gaussian beam of the wave type α in the solid at distance $\tilde{y}_3$ can be completely described by solving the paraxial wave equation (Huang 2005).

$$\mathbf{v}(\tilde{y}_3,\omega) = \frac{V(0)}{\sqrt{\det[A^P + B^P M(0)]}}\bar{\mathbf{d}} \times \exp\left(i\omega \left(\frac{\tilde{y}_3}{u_\alpha} + \frac{1}{2} Y^T \mathbf{M}^\alpha(\tilde{y}_3)\, Y \right) \right) \quad (1)$$

$$\mathbf{M}^\alpha(\tilde{y}_3) = \left[\mathbf{D}^P \mathbf{M}(0) + \mathbf{C}^P\right]\left[\mathbf{B}^P \mathbf{M}(0) + \mathbf{A}^P\right]^{-1} \quad (2)$$

In Eq. (1), the propagation matrices ($\mathbf{A}^P$,$\mathbf{B}^P$,$\mathbf{C}^P$,$\mathbf{D}^P$) in the solid are given by

$$\mathbf{A}^P = \begin{bmatrix} 1 & 0 \\ 0 & 1 \end{bmatrix},$$

$$\mathbf{B}^P = \frac{c_\alpha}{u_\alpha}\begin{bmatrix} (c_\alpha - 2C^\alpha)\tilde{y}_3 & -D^\alpha \tilde{y}_3 \\ -D^\alpha \tilde{y}_3 & (c_\alpha - 2E^\alpha)\tilde{y}_3 \end{bmatrix}, \quad (3)$$

$$\mathbf{C}^P = \begin{bmatrix} 0 & 0 \\ 0 & 0 \end{bmatrix}, \quad \mathbf{D}^P = \begin{bmatrix} 1 & 0 \\ 0 & 1 \end{bmatrix}$$

The 2×2 matrix $\mathbf{M}(0)$ is defined in the next section. In Eq. (3) c_α and u_α are magnitudes of phase and group velocities for a wave of type α, respectively, for a given propagation direction. The terms (C^α, D^α, E^α) represent the slowness surface curvatures (as measured in the slowness coordinates (x_1, x_2, x_3) along the refracted ray. In the isotropic case $C^\alpha = D^\alpha = E^\alpha = 0$. These curvature terms can be obtained by expanding the x_3 component of the slowness vector, $\mathbf{S}_\alpha$, (s_3^α) to the second order in the coordinates in the (x_1, x_2, x_3) form (Rudolph 1999).

$$s_3^\alpha = \frac{1}{c_\alpha} - \frac{u_I^\alpha}{c_\alpha} s_I^\alpha + K_{IJ}^\alpha s_I^\alpha s_J^\alpha \qquad (I,J = 1,2) \quad (4)$$

where (u_1^α, u_2^α) are the components of the group velocity vector, u_α, along the (y_1, y_2) axes, respectively, for a wave of type α. For an

isotropic solid $u^{\alpha}_1 = u^{\alpha}_2 = 0$. The matrix $\mathbf{K}^{\alpha}$ in Eq. (4) is given by

$$\mathbf{K}^{\alpha} = -\frac{1}{2}\begin{bmatrix} c_{\alpha} - 2C^{\alpha} & -D^{\alpha} \\ -D^{\alpha} & c_{\alpha} - 2E^{\alpha} \end{bmatrix} \quad (5)$$

For some simple type of anisotropic media the curvature terms can be expressed in analytical form. In general, they must be obtained numerically from the values of the slowness surfaces in the neighborhood of the refracted ray.

2.2 Modular Multi-Gaussian Beam Model

Using the approach of Wen and Breazeale (Wen and Breazeale 1988), by the superposition of 10 Gaussian beams, one can model the corresponding wave field of a circular piston source (of radius a). In this manner, Eq. (5) can be written as

$$\mathbf{v}^{\alpha}(\tilde{y}_3,\omega) = \sum_{n=1}^{10} \frac{V(0)\, A_n\, \bar{\mathbf{d}}^{\alpha}}{\sqrt{\det\left[\mathbf{A}^G + \mathbf{B}^G\,(\mathbf{M}(0))_n\right]}} \times \exp\left[i\omega\left(\frac{\tilde{y}_3}{u_{\alpha}} + \frac{1}{2}\mathbf{Y}^T\mathbf{M}^{\alpha}(\tilde{y}_3)\mathbf{Y}\right)\right] \quad (6)$$

where $(\mathbf{M}(0))_n = \frac{2iB_n}{\omega a^2}\mathbf{I}$, and A_n and B_n are ten complex constants (Wen and Breazeale 1988). Eq. (6) provides a highly efficient formulation for modeling the wave fields of ultrasonic transducers in very complex testing situations, and will be referred to as the "MMGB" model.

3. Local Properties of Slowness Surface

Equation (3) shows that the group velocity components and slowness surface curvatures are key parameters needed to define the propagation characteristics of a beam in an anisotropic solid. We examine the effects of these parameters when the transducer beam propagates directly into the symmetry plane of the anisotropic solid as shown in Fig. 1.

We use a local fitting procedure to extract the slopes and curvatures from numerical values of the slowness surface in the neighborhood of a particular direction. Equation (4) can be rewritten as

$$s_3 = s_0 + As_1 + Bs_2 + \left[C - \frac{1}{2s_0}\right](s_1)^2 + Ds_1s_2 + \left[E - \frac{1}{2s_0}\right](s_2)^2 \quad (7)$$

Sampling a small patch of the x_3 slowness surface near the direction N times will give rise to an N×5 over-determined system of equations. A least squares method can be used to compute the five unknown parameters of the slowness surface.

As an example of the use of this method, we consider the austenitic stainless steel whose properties are assumed to be transversely isotopic: C_{11}=C_{22}=262.7, C_{12}=98.2, C_{13}=C_{23}=145, C_{33}=216, C_{44}=C_{55}=129, C_{66}=82.3 GPa and ρ=8.12 g/cm^3. Figure 2(a) represents an example of slowness

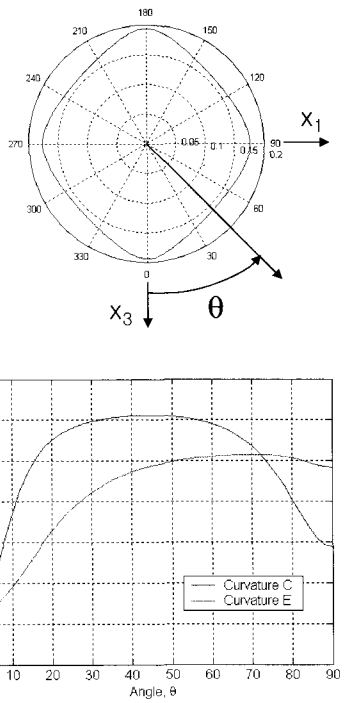

Fig. 2 (a) Slowness diagram in for austenite in the plane, (b) curvatures of qL wave for austenite in the x_1-x_3 plane

curve as a function of propagation direction in the x_1 - x_3 plane of the austenitic steel. Figure 2(b) plots the curvatures C and E for the qL wave. Note that for this example the parameter D is zero.

4. Results and Discussion

Here some results simulated by the MMGB model are presented. The studies show the effects of the slowness curvature changes on the beam propagation. We consider the qL wave radiating directly into austenitic steel along the x_3 axis which is along the 0° direction in Fig. 2(a), an axis of symmetry. Under this condition, along the y_3 axis the parameters for the qL wave are A^{qL} = B^{qL} = 0, C^{qL} = E^{qL} = -8mm/μs. Since this is an axis of material symmetry, there is no beam skewing (ψ=0 in Fig. 1). Fig. 3 shows 2-D beam profiles of the qL wave generated by a 5 MHz, 6.35 mm radius planar transducer. In order to see the effects of the curvature changes on the beam propagation more clearly, we artificially used three different curvature values: C=E=100%, 50%, and 0%. The 0% corresponds to the beam propagation in the isotropic solid with a slowness equivalent to for the anisotropic case. The profile is computed up to 100 mm in the solid. It is obvious that the beam spreads faster in the anisotropic cases than in the isotropic case. Shown in Fig. 4 are plots of the on-axis responses corresponding to the beam profiles shown in Fig. 3. It can be clearly seen how the beam profile moves away from the transducer face as the curvature of the slowness surface approach 0. Fig. 5 shows the cross-axis beam profiles at a distance $\tilde{y}_3$ where the on-axis response has its last peak. The last peak is found to occur at $\tilde{y}_3$ = 8.75 mm and $\tilde{y}_3$ = 39 mm for C=E=100% and 0%, respectively. The cross-axis response is unchanged even though the curvatures of the slowness surface changes significantly.

The anisotropy factor Λ/λ_Z for the qL wave beam radiation into the austenitic steel along the x_3 axis is given by (Newberry and Thompson 1989).

$$\frac{\Lambda}{\lambda_Z} = \frac{c_{44}}{c_{33}} + \frac{(c_{13}+c_{44})^2}{c_{33}(c_{33}-c_{44})} \tag{8}$$

For an isotropic material, c_{13} = c_{33} − $2c_{44}$, and Λ/λ_Z reduces to unity as it should. If we use the elastic constants of the austenitic steel considered in this study, Eq. (16) yields the anisotropy factor of 4.6. This means that when traveling a distance $\tilde{y}_3$ in the austenitic steel the equivalent distance becomes $(\Lambda/\lambda_Z)\tilde{y}_3$=4.6$\tilde{y}_3$ to achieve the same diffraction in an isotropic solid with a slowness equivalent to S_0 of the austenitic steel. If we refer to Fig. 4, this anisotropy factor is calculated as 39/3.75 ≈ 4.5 from the last peak distances for C=E=100% and 0% cases. Based on these comparisons, the MMGB model seems to provide very accurate diffraction effects.

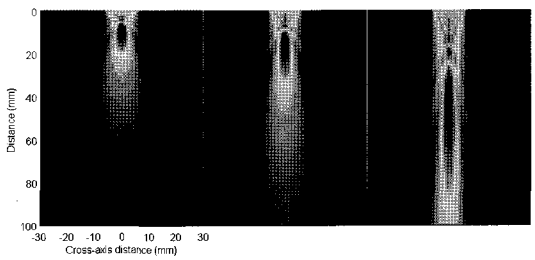

Fig. 3 2-D beam profiles of a 5 MHz, 6.35 mm diameterplanar transducer radiating directly into austenitic steel. Slowness curvatures change from C=E=100% to 0%. The 0% corresponds to the isotropic case.

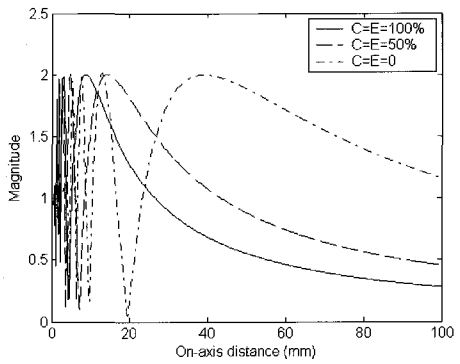

Fig. 4 On-axis responses corresponding to the beam profiles shown in Fig. 3

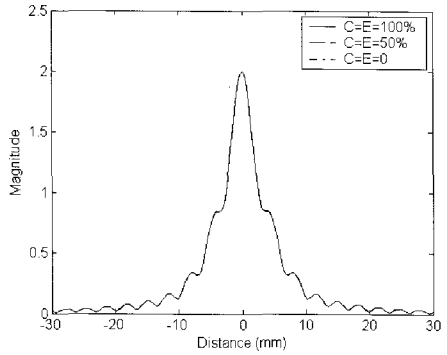

Fig. 5 Cross-axis beam profile at a distance $\tilde{y}_3$ where the on-axis response has its last peak

The MMGB model employed in this paper can be used to determine the transducer beam profile as it propagates in nonsymmetry directions within a symmetry plane. In this case, the anisotropic effects of beam skew and excess beam divergence due to diffraction should be observed at the same time. For this example, the solid will be taken to be the transversely isotropic austenite discussed in the previous section. Referring to Fig. 2, we can choose any directions except $\theta = 0°$ and $\theta = 90°$. In this example, however, we decided to use the propagation direction along $\theta = 72.3°$. The main reason for selecting this direction is that the curvatures C and E have the same value.

For the beam propagation in this direction, we rotate the coordinates (x_1, x_2, x_3) to the axis aligned with the beam, so that the slowness vector direction (or wave vector direction) always coincides with the x_3 axis. The slowness surface or the slowness curve in the $x_1 - x_3$ plane can then be obtained by rotating the stiffness tensor – which is originally defined in the material coordinate system – $\theta = 72.3°$ about the x_2 axis using the tensor transformation rules (Auld 1990).

Since the beam is normally incident, the propagating wave vector will be normal to the transducer face as well. The actual group velocity is normal to the slowness curve generated in the new coordinate system, and consequently the beam will skew.

The magnitude of the beam profile in the x-z plane is shown in Fig. 6. As a comparison, Fig. 6 includes an analogous situation of C=E=0 (isotropic case) and C=E=−150%. The same diffraction effects are observed as in the previous example. In other words, the beam pulls toward the transducer face as the values of C and E change from their original positive values to 0 and then negative values. This is consistent with the anisotropy factor for this case, Λ/λ_Z=0.9. The beam is seen to skew to the left of the inward normal direction. The approximate skew angle is $\psi = \arccos\left(1/\sqrt{A^2+B^2+C^2}\right) = -12.2°$, whereas the exact skew angle is found to be $\phi = -12.7°$. Based on these observations, the MMGB model correctly predicts both the beam skew and beam diffraction due to anisotropy. More complicated effects of the slowness surface are expected when the transducer beam propagates in a more general direction of anisotropic materials.

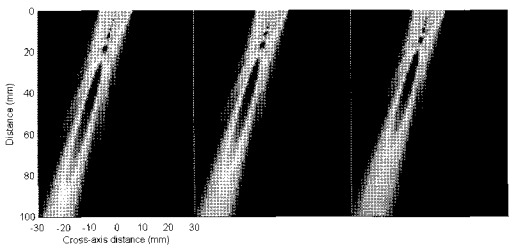

Fig. 6 2-D beam profile of a 5 MHz, 6.35 mm diameterplanar transducer radiating directly into austenitic steel. Slowness curvatures change from C=E=100% to C=E=−150%

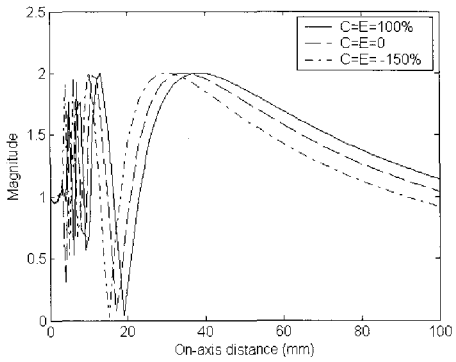

Fig. 7 On-axis responses corresponding to the beam profiles shown in Fig. 6

5. Conclusions

The slowness surface parameters such as slopes and curvatures are needed when simulating the beam propagation in anisotropic materials with models based on the paraxial approximation. The slopes of the slowness surface are related to the group velocity components in anisotropic materials, and it is well known that this causes beam skewing. We applied the MMGB model to look at the beam profile in transversely isotropic austenitic steels. The slowness curvatures also come into the MMGB model. We used a local fitting procedure to extract the curvatures from numerical values of the slowness surface in the neighborhood of a particular direction. Through parametric studies it was shown that the MMGB model correctly predicted the anisotropic effects of beam diffraction and beam skew. Therefore, the MMGB model can be efficiently used to predict the diffraction corrections in ultrasonic measurement models for anisotropic materials.

Acknowledgement

This work was supported by the 2006 nuclear R&D program administered by MOST.

References

Auld, B. A. (1990) Acoustic Fields and Waves in Solids, 2nd ed., Robert E. Krieger Publishing Co., Malabar, FL.

Huang, R., Schmerr, L. W. and Sedov, A. (2005) Multi-Gaussian Ultrasonic Beam Modeling for Multiple Curved Interfaces-An ABCD Matrix Approach, Research in Nondestructive Evaluation, Vol. 16, pp. 143-174

Jeong, H., Park, M.-C. and Schmerr, L. W. (2005) Application of a Modular Multi-Gaussian Beam Model to Some NDE Problems, Review of Progress in Quantitative Nondestructive Evaluation, Vol. 24, Eds. D. O. Thompson and D. E. Chimenti, pp. 986-993

Kim, H. J., Park, J.-S., Song, S.-J. and Schmerr, L. W. (2004) Modeling Angle Beam Ultrasonic Testing Using Multi-Gaussian Beams, Journal of Nondestructive Evaluation, Vol. 23, pp. 81-93

Kim, H.-J., Song, S.-J. and Schmerr, L. W. (2004) Modeling Ultrasonic Pulse-Echo Signals from a Flat-Bottom Hole in Immersion Testing Using a Multi-Gaussian Beam, Journal of Nondestructive Evaluation, Vol. 23, pp. 11-19

Lopez-Sanchez, A. L, Kim, H.-J., Schmerr, L. W. and Gray, T. A. (2006) Modeling the Response of Ultrasonic Reference Reflectors, Research in Nondestructive Evaluation, Vol. 17, pp. 49-69

Newberry, B. P. and Thompson, R. B. (1989) A Paraxial Theory for the Propagation of Ultrasonic Beams in Anisotropic Solids, J. Acoust. Soc. Am., Vol. 85, pp. 2290-2300

Norris, A. N. (1987) A Theory of Pulse Propagation in Anisotropic Elastic Solids, Wave Motion, Vol. 9, pp. 1-24

Ogilvy, J. A. (1986) Ultrasonic Beam Profiles and Beam Propagation in an Austenitic Weld Using a Theoretical Ray Tracing Model, Ultrasonics, Vol. 24, pp. 337-347

Papadakis, E. P. (1964) Diffraction of Ultrasound Radiating into an Elastically Anisotropic Medium, J. Acoust. Soc. Am., Vol. 36, pp. 414-422

Papadakis, E. P. (1966) Ultrasonic Diffraction Loss and Phase Change in Anisotropic Materials, J. Acoust. Soc. Am., Vol. 40, pp. 863-876

Rudolph, M. (1999) Ultrasonic Beam Models in Anisotropic Medi, Ph.D. Thesis, Iowa State University

Schmerr, L. W. and Sedov, A. (2003) A Modular Multi-Gaussian Beam Model for Isotropic and Anisotropic Media, Review of Progress in Quantitative Nondestructive Evaluation, Vol. 24, Eds. D. O. Thompson and D. E. Chimenti, pp. 828-835

Schmerr, L. W. (2000) A Multi-Gaussian Ultrasonic Beam Model for High Performance Simulations on a Personal Computer, Materials Evaluation, Vol. 58, pp. 882-888

Song, S.-J., Park, J.-S., Kim, Y. H., Jeong, H. and Choi, Y.-H. (2004) Prediction of Angle Beam Ultrasonic Testing Signals from a Surface Breaking Crack in a Plate Using Multi-Gaussian Beams and Ray Methods, Review of Progress in Quantitative Nondestructive Evaluation, Vol. 23, Eds. D. O. Thompson and D. E. Chimenti, pp. 110-117

Szabo, T. L. and Slobodnik, A. J. (1973) The Effect of Diffraction on the Design of Acoustic Surface Wave Devices, IEEE Trans. Sonics Ultrason., SU20, pp. 240-251

Wen, J. J. and Breazeale, M. A. (1988) A Diffraction Beam Field Expressed as the Superposition of Gaussian Beams, J. Acoustic. Soc. Am., Vol. 83, No. 5, 1752-1756